Neutron diffraction study of magnetic structure and successive 5*f* electronic transition in the itinerant antiferromagnet $NpRhGa_5$

Shintaro Jonen,[1,*] Naoto Metoki,[1,2] Fuminori Honda,[1] Koji Kaneko,[1] Etsuji Yamamoto,[1] Yoshinori Haga,[1] Dai Aoki,[3] Yoshiya Homma,[3] Yoshinobu Shiokawa,[1,3] and Yoshichika Ōnuki[1,4]

[1]*Advanced Science Research Center, Japan Atomic Energy Agency, Tokai, Naka, Ibaraki 319-1195, Japan*

[2]*Department of Physics, Tohoku University, Sendai 980-8578, Japan*

[3]*Institute for Materials Research, Tohoku University, Oarai, Ibaraki 311-1313, Japan*

[4]*Graduate School of Science, Osaka University, Toyonaka, Osaka 560-0043, Japan*

(Received 8 July 2005; revised manuscript received 18 April 2006; published 17 October 2006)

Neutron diffraction experiments have been carried out in a single crystal of $NpRhGa_5$ in order to reveal the magnetic structure and 5*f* electronic state. This material exhibits two successive antiferromagnetic transitions at $T_{N1}=36$ K and $T_{N2}=33$ K. An A-type antiferromagnetic structure with the propagation vector $\vec{q}=(0\ 0\ 1/2)$, appears below T_{N1}. We found a remarkable change in the moment direction at T_{N2}, namely, the Np moment is parallel to the *c* axis for $T_{N2}<T<T_{N1}$ (AF1), but parallel to the $\langle 1\ 1\ 0\rangle$ direction in the basal plane for $T<T_{N2}$ (AF2). The magnitude of the magnetic moment also exhibits a remarkable and discontinuous change at T_{N2}, indicating the moment reorientation is associated with a change of the 5*f* electronic state. This electronic transition might be the consequence of the competition between the magnetic and/or quadrupolar interaction in the low-moment (AF1) and high-moment (AF2) states. The observed magnetic form factor indicates a dominant contribution from the orbital moment, with a small reduction from the Np^{3+} free ion state.

DOI: 10.1103/PhysRevB.74.144412 PACS number(s): 75.25.+z, 75.30.Kz, 71.27.+a

I. INTRODUCTION

The exotic electronic properties of 115 compounds of ATX_5, where A=rare earth or actinide, T=transition metal, and X=In or Ga, have been attracting much attention since the discovery of unconventional superconductivity in rare-earth $CeTIn_5$[1–3] and in $Pu(Co,Rh)Ga_5$.[4,5] ATX_5 crystallizes in the tetragonal $HoCoGa_5$-type structure ($P4/mmm$) that consists of a sequential stacking of AX_3 layers with the $AuCu_3$ structure and transition metal layers along the tetragonal *c* axis, as shown in Fig. 1. The intensive investigation of these materials is certainly motivated by the unconventional superconductivity observed in Ce[1–3] and Pu-based[4–7] compounds, and by their interesting magnetic properties, particularly a remarkable variety of magnetic structures in $UTGa_5$[8–10] and $NpTGa_5$.[11,12]

Neutron diffraction experiments revealed that $UNiGa_5$ has a G-type antiferromagnetic structure with the propagation vector $\vec{q}=(1/2\ 1/2\ 1/2)$,[8] while $UPdGa_5$ and $UPtGa_5$ have an A-type antiferromagnetic order with $\vec{q}=(0\ 0\ 1/2)$.[8–10] This difference is unusual because the nearest-neighbor interaction has a different sign, although the electronic structures are almost identical.

Among the Np-based 115 compounds, $NpCoGa_5$ has an A-type antiferromagnetic structure below $T_N=46$ K,[11,13,14] whereas $NpFeGa_5$ is a C-type antiferromagnet with $\vec{q}=(1/2\ 1/2\ 0)$ ($T_N=118$ K), where both Np and Fe atoms have magnetic moments.[12,15–17] Thus, a wide variety of magnetic structures are realized in U- and Np-based 115 compounds.

Recently, a high-quality single crystal of $NpRhGa_5$ has been grown.[17] This is an isostructural derivative of the heavy-fermion superconductor $PuRhGa_5$.[5] The magnetic, electrical transport, and thermodynamical studies in $NpRhGa_5$ revealed an antiferromagnetic order with two successive phase transitions reported by Aoki *et al.* with $T_{N1}=36$ K and $T_{N2}=32$ K,[17] and Colineau *et al.* with $T_{N1}=37$ K and $T_{N2}=32$ K.[18] The magnetic susceptibility obeys the Curie-Weiss law at high temperatures and shows an anomalous behavior in the vicinity of the transition temperatures.[17–19] The anomalies were also observed in the specific heat measurements,[17–19] where the transition at T_{N2} is concluded to be first-order from a sharp anomaly peak. A recent ^{237}Np Mössbauer spectroscopy study showed the reorientation of moment with respect to the principal axis.[18] Colineau *et al.* suggested the change of moment direction from the *c* axis to the basal plane at T_{N2},[18] which should be directly observed by neutron diffraction. Furthermore, the observed hyperfine field around the ordering temperature showed a large error bar due to the thermal effect.[18] To un-

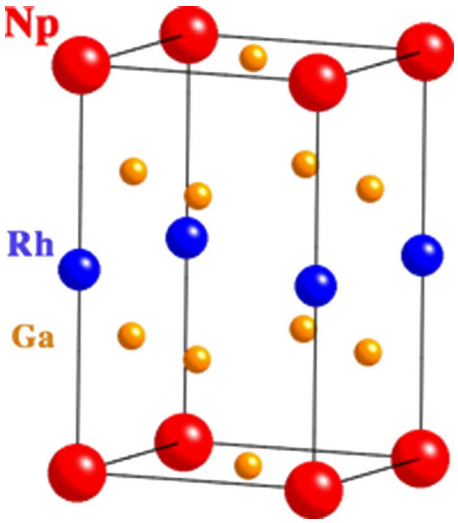

FIG. 1. (Color online) Crystal structure of $NpRhGa_5$.

derstand the nature of this successive phase transition in $NpRhGa_5$, a single-crystal neutron diffraction experiment is important.

In this paper we report the magnetic structure and $5f$ electronic state of $NpRhGa_5$ by neutron diffraction measurements.

II. EXPERIMENT

Neutron diffraction experiments have been carried out using the thermal and cold triple-axis spectrometers TAS-1, TAS-2, and LTAS installed at the research reactor JRR-3 in the Japan Atomic Energy Agency (JAEA).

The magnetic reflections were searched using the TAS-2 spectrometer. An incident beam with the dimensions of 20×200 mm^2 was monochromatized and analyzed with vertically bent pyrolytic graphite (PG) crystals. Higher order contaminations were effectively removed to less than 10^{-5} of the primary beam intensity via a 12-cm-thick PG filter and a multilayer Ni/Ti $2Q$ supermirror that has a cutoff energy of $\sim$35 meV, in the T2 beam guide.

The crystal and magnetic structures have been studied using the TAS-1 spectrometer. To reduce the systematic error of integrated intensity, the neutron beam was monochromatized and analyzed using a flat PG monochromator. Relatively high energy beams of $E=33$ and 40 meV were used to measure the integrated intensity of many reflections up to $\sin\theta/\lambda=0.5$ Å^{-1}. The integrated intensity of 58 and 46 reflections of nuclear and magnetic diffraction peaks, respectively, were measured in the longitudinal scans on the $(h\ 0\ l)$ and $(h\ h\ l)$ scattering planes. Higher-order contaminations were removed via the 12-cm-thick PG filter and subtracted as a background by comparing with the result in the paramagnetic phase.

Experiments under high magnetic field up to 10 T were carried out on the cold triple-axis spectrometer LTAS to study the single-domain sample. A vertical field was applied with the use of a liquid-^{4}He-free superconducting magnet for neutron scattering developed by JAEA.[20] The neutron beam was monochromatized and analyzed via vertically bent PG crystals at 5 meV. Higher order contaminations were filtered using a 20-cm-thick Be block, cooled down to 20 K.

All experiments were carried out in the triple-axis mode without collimators for the scattered beam to improve the efficiency of diffraction intensity. The background from the sample cell, cryostat, and magnet was removed using a pair of beam slits.

A high-quality single-crystal sample of $NpRhGa_5$ was grown by the Ga-flux method. The details of sample preparation are given elsewhere.[17] A large single-crystal sample with dimensions of $5\times5\times2$ mm^3 was sealed in a tiny aluminum tube in a He atmosphere. The sample tube was encapsulated in an aluminum cell with He exchange gas and cooled down to 3 K using a closed-cycle refrigerator.

The present single-crystal sample exhibits a considerable absorption and extinction effect. The absorption correction was applied numerically in all of the collected integrated intensity data by the Meulenaer and Tompa (analytical) method,[21,22] using the software PLATON.[23,24] After the application of absorption correction, primary and secondary extinction corrections were applied by the Becker and Coppens method.[25–27]

TABLE I. The observed integrated intensity (I_o) at $E=33$ meV and $T=3$ K, the observed intensity after the absorption correction (I_{abs}), the calculated intensity with the kinematical model (I_{kin}), and that with the extinction correction (yI_{kin}).

Q	I_o	I_{abs}	I_{kin}	yI_{kin}
(0 0 1)	17.88	43.00	55.00	54.18
(0 0 2)	4.47	9.87	0.04	0.04
(0 0 3)	532.60	1082.05	2399.41	1016.91
(0 0 4)	407.25	766.00	1748.93	798.09
(0 0 5)	173.41	304.82	396.46	295.27
(1 0 0)	148.69	234.85	294.08	267.56
(1 0 1)	15.55	25.62	20.79	20.60
(1 0 2)	88.44	161.56	188.42	169.97
(1 0 3)	9.43	18.72	12.21	12.10
(1 0 4)	57.89	111.32	123.14	111.41
(1 0 5)	5.93	10.62	9.13	9.05
(1 0 6)	62.50	105.15	106.09	96.29
(2 0 0)	921.41	1464.45	5177.95	1455.37
(2 0 1)	12.45	20.25	17.73	17.51
(2 0 2)	1.67	2.87	0.02	0.02
(2 0 3)	437.77	801.02	1787.49	792.53
(2 0 4)	341.22	664.53	1502.61	701.64
(2 0 5)	160.83	295.33	374.19	279.68
(3 0 0)	64.15	104.48	115.41	104.67
(3 0 1)	11.91	19.68	9.46	9.37
(3 0 2)	57.65	99.15	110.76	100.43
(3 0 3)	9.57	17.41	8.90	8.82
(3 0 4)	46.66	89.70	106.11	96.19

III. RESULTS

A. Crystal structure

The integrated intensity of nuclear reflections has been measured to determine the scale factor, which is necessary to determine the magnitude of magnetic moment. The Bragg reflection revealed a tetragonal-type crystal structure with the lattice parameters $a=4.291$ Å and $c=6.833$ Å at 3 K. The results are in close agreement with those obtained in a polycrystalline x-ray diffraction experiment.[18] In our analysis, the integrated intensity has been calculated using the tetragonal $HoCoGa_5$-type crystal structure with $z_{Ga}=0.2987$, reported previously by Colineau *et al.*[18]

The data correction of absorption and the extinction effect is shown in Table I. I_o represents the observed integrated intensity data, measured by longitudinal scans in the $(h\ 0\ l)$ scattering plane. I_{abs} is the corrected observed data after the application of absorption correction.

I_{kin} represents the nuclear diffraction intensity calculated by the theoretical kinematical model, and yI_{kin} is the same

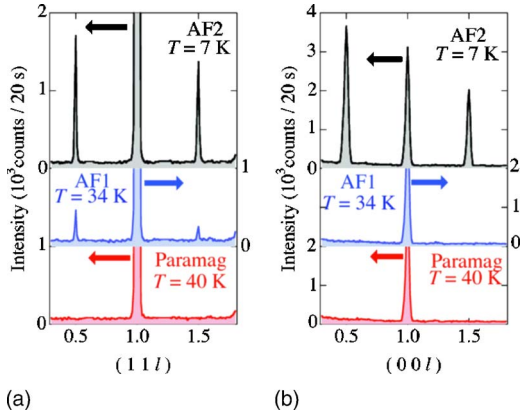

FIG. 2. (Color online) Temperature dependence of the line-scan profile in $NpRhGa_5$, along (a) (1 1 l) and (b) (0 0 l) measured at T=7 K (AF2), 34 K (AF1), and 40 K (paramagnetic).

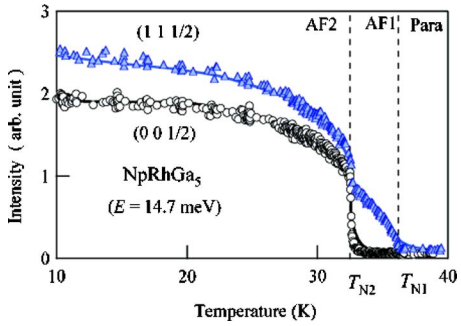

FIG. 3. (Color online) The temperature dependence of (1 1 1/2) (△) and (0 0 1/2) (○) magnetic diffraction intensity. T_{N1} represents an antiferromagnetic order temperature. At T_{N2}, a sharp increase in (1 1 1/2) and (0 0 1/2) magnetic peaks indicates a first-order transition, accompanied by reorietation of Np moments.

calculation with an application of extinction correction. The refinement of extinction correction was carried out by minimizing the deviation $R=\Sigma|F_o^2-yF_k^2|/\Sigma F_o^2$, where F_o represents the observed structure factor after the application of absorption correction, F_k is the theoretical structure factor calculated by a kinematical model, and y is the extinction correction parameter. The mosaic block size and the mosaic spread, estimated by analysis of primary and secondary extinction correction, are 5×10^{-6} cm and 0.11°, respectively. The mosaic spread is consistent with our result in rocking curve measurement, which provides an instrumental resolution-limited peak width of 0.4°.

After the application of extinction correction, the theoretical model reproduces well the experimental data, where we obtained R=0.04 and 0.10 by the least-squares fitting, for energies E=33 and 40 meV, respectively. No significant extinction correction was necessary for the integrated intensity of the magnetic reflections because of the weak intensity.

B. Magnetic structure

Figure 2 shows the temperature dependence of the neutron diffraction profiles along the (a) (1 1 l) and (b) (0 0 l) scan directions, for $0.3<l<1.8$ reciprocal lattice unit (r.l.u.). Below T_{N1}=36 K, the superlattice peaks were observed at (1 1 1/2) and (1 1 3/2), indicating an antiferromagnetic structure with the propagation vector $\vec{q}$=(0 0 1/2) for both of the magnetically ordered phases. No magnetic peak was observed at (1/2 1/2 1/2) and (1/2 1/2 0). The observed structure can be described with a ferromagnetic layer on a basal plane, stacked along the tetragonal c axis in an antiferromagnetic sequence. The absence of a magnetic peak in the (0 0 l) direction at T=34 K indicates that the Np magnetic moments are oriented along the c axis for $T_{N2}<T<T_{N1}$ (AF1). This A-type antiferromagnetic structure is the same as that of $NpCoGa_5$,[11] $UPdGa_5$,[9,10] and $UPtGa_5$.[10] The identical magnetic structures are reasonably understood from the electronic structures of the compounds; these isoelectronic compounds have very similar cylindrical Fermi surfaces.[28–31] In the AF2 phase below T_{N2}, half-integer superlattice peaks were observed in the (0 0 l) direction, indicating an existence of the in-plane component of antiferromagnetic moment below T_{N2}.

The temperature dependence of (0 0 1/2) and (1 1 1/2) antiferromagnetic Bragg intensity is shown in Fig. 3. Below T_{N1}, the antiferromagnetic peak (1 1 1/2) shows a continuous increase in intensity with decreasing temperature, whereas the intensity at (0 0 1/2) has not been observed in AF1. At T_{N2}, a sudden increase in peak intensity for (1 1 1/2) and a sharp increase in (0 0 1/2) peak intensity have been observed, indicating a first-order transition at the moment of reorientation temperature T_{N2}.

From the results of the magnetic profiles shown in Fig. 2, we propose models of magnetic structures for the AF1 and AF2 phases, as shown in the inset of Fig. 4. In AF1, the direction of the Np moment is parallel to the c axis, and the Np moment is in the basal plane in AF2.

We summarize the integrated intensity of the antiferromagnetic reflections in the (h 0 l) scattering plane for AF1 and AF2, shown in the upper and lower panel of Fig. 4, respectively. The magnetic reflection intensity of a collinearly ordered single-ion system for an unpolarized neutron beam can be written as

$$I(\mathbf{Q}) \propto \mu^2 f^2(\mathbf{Q}) |F_M(\mathbf{Q})|^2 \langle \sin^2 \alpha \rangle \mathcal{L}(\theta), \tag{1}$$

where μ is the magnetic moment, $F_M(\mathbf{Q})$ is the magnetic structure factor, $f(\mathbf{Q})$ is the magnetic form factor, $\langle \sin^2 \alpha \rangle$ is the angle factor where α is the angle between the ordered magnetic moments and the scattering vector $\mathbf{Q}$, and $\mathcal{L}(\theta)$ $=1/\sin 2\theta$ is the Lorentz factor for the present case. The magnetic structure factor $F_M(\mathbf{Q})$ is unity for our model structures. The experimental intensity, corrected by absorption correction, are denoted by solid circles for both AF1 and AF2. They can be well reproduced by the model calculation, indicated by solid bars as shown in Fig. 4. The Np magnetic moments extracted from this analysis are μ=0.89(4) μ_B at T=3 K and μ=0.32(10) μ_B at T=34 K. The Np moment obtained for AF2 are consistent with that of the Mössbauer experiment.[18] The in-plane direction of magnetic moment cannot be determined from the present result due to the domain structure. As described later we have confirmed that the

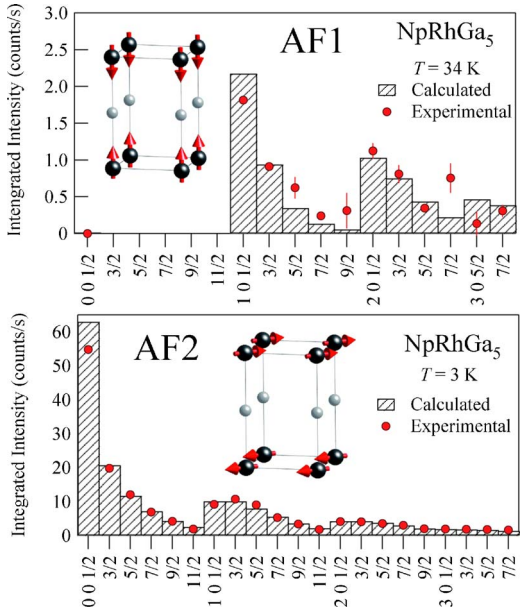

FIG. 4. (Color online) The absorption-corrected experimental integrated intensity of magnetic reflections at T=34 K (AF1) and T=3 K (AF2). The Np magnetic moments are μ=0.32(10) μ_B at T=34 K and μ=0.89(4) μ_B at T=3 K. The inset figures represent the magnetic structure of $NpRhGa_5$, where Np is the unique magnetic atom. In AF1, the Np moment is parallel to the c axis. In AF2, the moment is parallel to the ⟨1 1 0⟩ direction in the basal plane. Ga atoms are not shown for clarity.

moment direction is parallel to the ⟨1 1 0⟩ direction on the basal plane.

The temperature dependence of the magnetic moment is shown in Fig. 5. The magnetic moment is extracted by normalizing the antiferromagnetic intensity with angle and Lorentz factors using Eq. (1). The most remarkable point is the presence of a discontinuous change in magnetic moment, from 0.38 μ_B to 0.62 μ_B, observed at T_{N2}. Therefore, the first-order transition at T_{N2} is not a simple reorientation of the magnetic moment but is accompanied with the strong enhancement in the magnitude of the magnetic moments. As

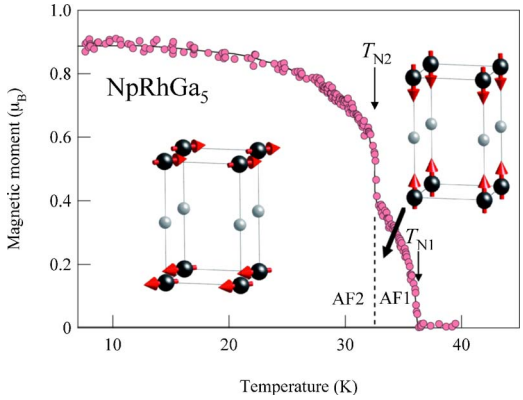

FIG. 5. (Color online) Temperature dependence of Np magnetic moment and the magnetic structure of $NpRhGa_5$. The magnetic moment exhibits a sharp jump accompanied by a reorientation of moments at T_{N2}, indicating a change of $5f$ electronic state.

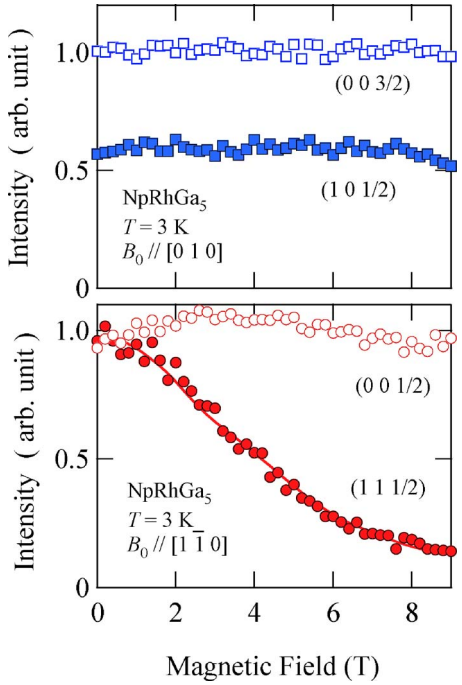

FIG. 6. (Color online) Field dependence of the magnetic peak intensity at T=3 K (AF2). The data obtained with field along the [0 1 0] and [1 $\bar{1}$ 0] directions are shown in the upper and lower panel, respectively. The solid line is a guide to the eye.

described in the following discussion part, we conclude that this transition is a consequence of the change of the $5f$ electronic state.

The direction of Np moments in the AF2 phase has been determined by analysis of the magnetic domain structure under a magnetic field. We have performed the neutron diffraction measurements with an external magnetic field B_0 up to 10 T applied in the basal plane. The field dependence of the magnetic diffraction intensity is shown in Fig. 6. With the field applied along the [0 1 0] direction, no significant change in the (1 0 1/2) and (0 0 3/2) intensity has been observed. This means that a multidomain structure is maintained in this field direction. For a magnetic field parallel to the [1 $\bar{1}$ 0] direction, however, the (1 1 1/2) intensity is reduced to 14% for $B_0 > 8$ T in comparison with that for $B_0 = 0$. The observed reduction is consistent with the model calculation (21%) for a single-domain structure with the antiferromagnetic moment perpendicular to the field, namely, in the scattering plane. In the multidomain case the integrated intensity [Eq. (1)] is calculated by the average of angle factor $\langle \sin^2 \alpha \rangle$ over domains. Therefore, a reduction in intensity in the model calculation was obtained when we calculated the angle factor for the single domain case. The (0 0 1/2) intensity remains constant, indicating that the magnitude of magnetic moment shows no field dependence. From these results we conclude that the ⟨1 1 0⟩ direction is the magnetic easy axis in AF2.

C. Magnetic form factor

The magnetic form factor $f(\mathbf{Q})$ is a direct measure of the magnetization distribution. $f(\mathbf{Q})$ can be described as the sum

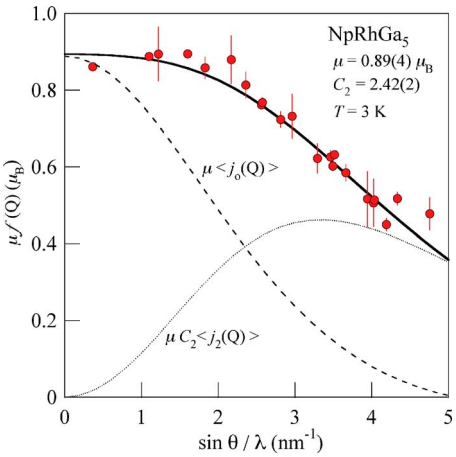

FIG. 7. (Color online) $\mu f(\mathbf{Q})$ of $NpRhGa_5$ at $T=3$ K. The circles are the results of the absorption-corrected magnetic diffraction intensity as a function of $Q/4\pi=\sin\theta/\lambda$. The solid line is the best fit of calculated magnetic form factor using Eq. (5) with μ and C_2 as fitting parameters. The dashed and dotted lines show the calculated curves for $\mu\langle j_0\rangle$ and $\mu C_2\langle j_2\rangle$ terms, respectively.

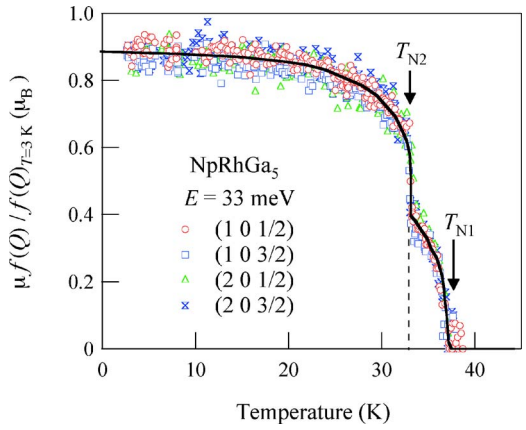

FIG. 8. (Color online) Temperature dependence of $\mu f(\mathbf{Q})$ divided by $f(\mathbf{Q})$ at $T=3$ K for antiferromagnetic reflections in a wide $\mathbf{Q}$ range. The solid line is a guide to the eye.

of the spin and orbital contributions $f_S(\mathbf{Q})$ and $f_L(\mathbf{Q})$,[32]

$$\mu f(\mathbf{Q}) = \mu_S f_S(\mathbf{Q}) + \mu_L f_L(\mathbf{Q}), \tag{2}$$

where μ_S and μ_L are the spin and orbital moments, respectively. $f(\mathbf{Q})$ can be expanded on the basis of spherical Bessel functions. Within the dipole approximation, the spin and orbital components are given,

$$f_S(\mathbf{Q}) \sim \langle j_0\rangle, \tag{3}$$

$$f_L(\mathbf{Q}) \sim \langle j_0\rangle + \langle j_2\rangle. \tag{4}$$

By substituting Eqs. (3) and (4) into Eq. (2), we obtain

$$\mu f(\mathbf{Q}) = \mu(\langle j_0\rangle + C_2\langle j_2\rangle), \tag{5}$$

where $\mu=\mu_S+\mu_L$ and $C_2=\mu_L/\mu$.

The experimental $\mu f(\mathbf{Q})$, calculated from absorption corrected magnetic intensity (Fig. 7), has been decomposed using Eq. (5). The solid curve in Fig. 7 is a result of least-squares fitting with two adjustable parameters μ and C_2. The results of μ, C_2, and the decomposition in the spins and orbital components are shown in Table II. The observed magnetic form factor with $\mu=0.89(4)$ μ_B and $C_2=2.42(2)$ at $T=3$ K indicates the dominant contribution of orbital moment, with $-\mu_L/\mu_S=1.71$.

The estimated $C_2=2.42$ is slightly different from the Np^{3+} free ion value ($C_2=2.33$). A recent result of de Hass-van Alphen (dHvA) experiments by Aoki *et al.*[28] reported that the Fermi surface topology can be well explained by band structure calculation with itinerant $5f$ electrons. Therefore, the small reduction of orbital contribution might be associated with a partial quenching of μ_L where the $5f$ electrons show an itinerant character.[32]

TABLE II. Spin (μ_S) and orbital (μ_L) components of magnetic moment in AF1 and AF2 phases, and Np^{3+} free ion case.

	μ (μ_B)	μ_S (μ_B)	μ_L (μ_B)	$-\mu_L/\mu_S$	C_2
$NpRhGa_5$ (34 K)	0.32(10)	−0.45	0.77	1.71	2.42
$NpRhGa_5$ (3 K)	0.89(4)	−1.26	2.15	1.71	2.42
Np^{3+}				1.75	2.33

The measurement of the magnetic form factor in the AF1 phase was quite difficult, because the AF1 phase exists only in a very narrow temperature range, where the magnetic peak intensity is rather weak and highly sensitive to sample temperature. Furthermore, the absence of low-$\mathbf{Q}$ peaks such as (0 0 1/2) and (0 0 3/2) hinders a good analysis of the magnetic form factor to evaluate μ and C_2 parameters. Therefore, we tried to determine if the magnetic form factor exhibits a significant temperature dependence in comparison with the one for the AF2 phase.

Figure 8 shows the temperature dependence of $\mu f(\mathbf{Q})$ normalized with $f(\mathbf{Q})$ at $T=3$ K, $\mu f(\mathbf{Q})/f(\mathbf{Q})_{T=3\text{ K}}$. The data from several antiferromagnetic Bragg intensities are plotted in the same scale on the basis of Eq. (1). As shown in Fig. 8, all data points of antiferromagnetic reflections in a wide $\mathbf{Q}$ range are on a universal curve. Despite the high statistical fluctuation observed in all curves, the magnetic form factor $f(\mathbf{Q})$ does not show a significant change with temperature even below and above T_{N2}. Thus, the magnetic form factor in the AF1 phase would be similar to the one for the AF2 phase. From these results we analyzed the data of the magnetic form factor measurement in the AF1 phase assuming $C_2=2.42$, the same value as in the AF2 phase, and obtained the magnetic moment $\mu=0.32$ (10)μ_B. These values are also summarized in Table II.

IV. DISCUSSION

The unusual temperature dependence of the magnetic susceptibility[17] shown in Fig. 9 can be qualitatively explained in terms of the magnetic structures determined by the present study. The magnetic susceptibility along the c axis, $\chi\|c$, is larger than that perpendicular to the c axis, $\chi\perp c$, in the paramagnetic phase. Below T_{N1}, $\chi\|c$ steeply decreases,

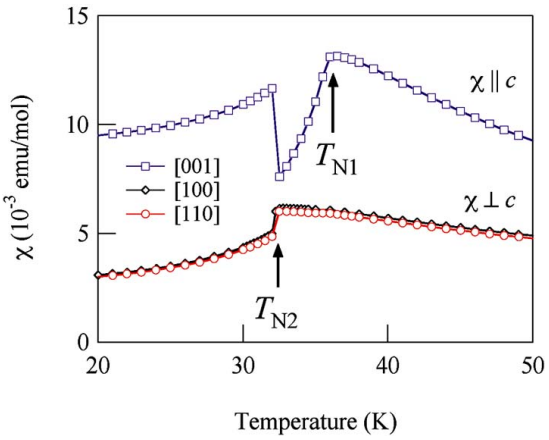

FIG. 9. (Color online) The magnetic susceptibility of $NpRhGa_5$ in the vicinity of the magnetic transition temperatures (Ref. 17).

whereas $\chi \perp c$ remains almost constant without any anomaly at T_{N1}. This behavior is consistent with the antiferromagnetic structure in the AF1 phase ($T_{N2} < T < T_{N1}$) with the Np moment along the c axis. Thus, the c axis is the magnetic easy axis. In the AF2 phase the magnetic anisotropy switches to the in-plane easy axis. Therefore, we expect that some part of $\chi \| c$ is recovered and some part of $\chi \perp c$ is suppressed, as observed at T_{N2}.

The most remarkable feature in the present neutron diffraction study on $NpRhGa_5$ is the discontinuous change in the magnetic moment observed at T_{N2}. We conclude that this is a first-order transition between the low-moment and high-moment $5f$ electronic states, accompanying the reorientation of the moment direction, where $\mu \| c$ is the low-moment state at high temperatures (AF1) and $\mu \perp c$ is the high-moment state at low temperatures (AF2).

The successive magnetic order and the transition of the $5f$ electronic state can be qualitatively understood on the basis of a localized $5f$ electron model. The recent ^{237}Np Mössbauer study clarified the trivalent Np^{3+} state in $NpTGa_5$.[14,18] The J multiplet with $5f^4$ ($J=4$) configuration splits into two doublets with Γ_5 symmetry and five singlet states under a crystalline electric field (CEF) with tetragonal point symmetry. The CEF level scheme of $NpCoGa_5$ has been studied from the temperature dependence of the magnetic susceptibility, based on a mean field Hamiltonian with CEF and an anisotropic exchange interaction.[13] Aoki *et al.* proposed a doublet ground state with a singlet first excited state at 87 K. The level scheme is shown in Fig. 10. The other levels have excitation energies of more than 1000 K; thus, we can ignore these high energy levels when we discuss magnetic properties below room temperature. The magnetic entropy of $R \ln 2$ relative to T_N is consistent with the doublet ground state.[11] The observed magnetic moment of approximately

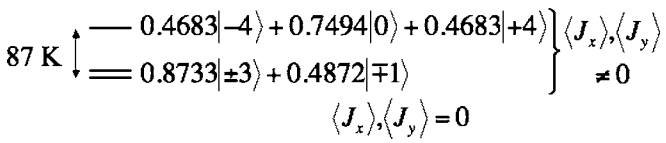

FIG. 10. Low-energy CEF scheme in $NpCoGa_5$ (Ref. 13).

0.8 μ_B/Np[11] is somewhat smaller than that expected from the CEF model, 1.25 μ_B/Np.[13] However, the reduction of the magnetic moment is reasonable because of the itinerant character of the $5f$ electrons in $NpCoGa_5$.

The doublet ground state has only J_z observed in $NpCoGa_5$, as easily understood from the wave function

$$|\phi_0\rangle = 0.8733|\pm 3\rangle + 0.4872|\mp 1\rangle. \tag{6}$$

The symmetry of the wave function does not allow the in-plane components J_x and J_y,

$$\langle \phi_0|J_x|\phi_0\rangle = \langle \phi_0|J_y|\phi_0\rangle = 0. \tag{7}$$

This characteristic is the origin of the strong uniaxial magnetic anisotropy in $NpCoGa_5$. The in-plane component of $NpRhGa_5$ in the AF2 phase can be produced only by mixing the excited singlet state

$$|\phi_1\rangle = 0.4682|-4\rangle + 0.7494|0\rangle + 0.4682|+4\rangle \tag{8}$$

into the doublet ground state.

The off-diagonal order accompanies the in-plane magnetic component

$$g_J \sum \langle \phi_0|J_x + J_y|\phi_1\rangle \mu_B = 1.2\mu_B, \tag{9}$$

where g_J is the Landé g factor (3/5 for Np^{3+}).

Note that the CEF level scheme of $NpRhGa_5$ is expected to be very similar to that of $NpCoGa_5$ because of the similarity in electronic structure; they are isoelectronic compounds, having very similar cylindrical Fermi surfaces,[28,29,33–35] and the antiferromagnetic propagation vector $\vec{q}=(0\ 0\ 1/2)$ is also identical.[11]

Recently, this scenario was discussed theoretically by Kiss and Kuramoto.[36] They succeeded to explain the magnetic structure and the magnetic phase diagram of $NpTGa_5$ (T=Co, Rh, and Ni) in terms of the mean field theory based on a localized model with CEF, and dipole and quadrupole interactions. The most interesting result in their theoretical study is the prediction of coexistence of ferroquadrupole order and antiferromagnetic order in $NpRhGa_5$. Therefore the competing magnetic and quadrupolar interactions in the multi-$5f$ orbital might be the origin of the successive magnetic transition.

Contrary to the rather simple and classical arguments based on the localized $5f$ electron picture mentioned above, it was suggested that $NpRhGa_5$ is an itinerant antiferromagnet from dHvA experiments.[28] A slight suppression of $-\mu_L/\mu_S$, observed in the present study, might be somewhat indicative for the itinerant behavior of $5f$ electron in $NpRhGa_5$. To date, there has been no clear explanation for the magnetic structure and the successive transition in $NpRhGa_5$ from the band theory. A comparison of the total energy calculation for various types of ordering[35] would give a clue to the understanding of the unusual transition of the $5f$ electronic state, although calculations for finite temperatures would be very hard. Opahle *et al.*[37] has reported the importance of orbital polarization correction in their calculation for $NpCoGa_5$. We may expect some competing effect of the Fermi surfaces originating from different bands. Recently, a theoretical study based on j-j coupling scheme has been pro-

posed to describe the magnetic structure of NpTGa$_5$.[38] The successive magnetic order associated with the transition of the 5f electronic state appearing in the family of 115 compounds would shed light on this issue.

V. CONCLUSIONS

NpRhGa$_5$ exhibits an antiferromagnetic order with the propagation $\vec{q}=(0\ 0\ 1/2)$. The moment direction is parallel to the c axis for 33 K$<T<$36 K, and it is in-plane along $\langle 110\rangle$ for $T<33$ K. The moment sizes are 0.32(10) μ_B at 34 K and 0.89(4) μ_B at 3 K. A marked discontinuous change of the magnetic moment has been observed at the first-order transition at $T_{N2}=33$ K. It has been observed that the magnetic form factor has a dominant orbital moment. The small suppression of orbital contribution might be due to the itinerant character of a 5f electron state. The successive magnetic order is discussed in terms of the localized model. We conclude that this is associated with the transition of the 5f electronic state between low-moment and high-moment states, which suggests the competing magnetic and quadrupolar interactions between different 5f orbitals.

ACKNOWLEDGMENTS

We thank Y. Kuramoto, A. Kiss, H. Onishi, T. Hotta, H. Yasuoka, E. Colineau, S. Wilkins, F. Wastin, and G. H. Lander for helpful discussions. This study was financially supported by a Grant-in-Aid for Scientific Research from the Japanese Ministry of Energy, Culture, Sports, and Technology (No. 16740212).

*Electronic address: jonen.shintaro@jaea.go.jp

[1] H. Hegger, C. Petrovic, E. G. Moshopoulou, M. F. Hundley, J. L. Sarrao, Z. Fisk, and J. D. Thompson, Phys. Rev. Lett. **84**, 4986 (2000).
[2] R. Movshovich, M. Jaime, J. D. Thompson, C. Petrovic, Z. Fisk, P. G. Pagliuso, and J. L. Sarrao, Phys. Rev. Lett. **86**, 5152 (2001).
[3] C. Petrovic, R. Movshovich, M. Jaime, P. G. Pagliuso, M. F. Hundley, J. L. Sarrao, Z. Fisk, and J. D. Thompson, Europhys. Lett. **53**, 354 (2001).
[4] J. L. Sarrao, L. A. Morales, J. D. Thompson, B. L. Scott, G. R. Stewart, F. Wastin, J. Rebizant, P. Boulet, E. Colineau, and G. H. Lander, Nature (London) **420**, 297 (2002).
[5] F. Wastin, P. Boulet, J. Rebizant, E. Colineau, and G. H. Lander, J. Phys.: Condens. Matter **15**, S2279 (2003).
[6] H. Sakai, Y. Tokunaga, T. Fujimoto, S. Kambe, R. E. Walstedt, H. Yasuoka, D. Aoki, Y. Homma, E. Yamamoto, A. Nakamura, Y. Shiokawa, K. Nakajima, Y. Arai, T. D. Matsuda, Y. Haga, and Y. Ōnuki, J. Phys. Soc. Jpn. **74**, 1710 (2005).
[7] Y. Haga, D. Aoki, T. D. Matsuda, K. Nakajima, Y. Arai, E. Yamamoto, A. Nakamura, Y. Homma, Y. Shiokawa, and Y. Ōnuki, J. Phys. Soc. Jpn. **74**, 1698 (2005).
[8] Y. Tokiwa, Y. Haga, N. Metoki, Y. Ishii, and Y. Ōnuki, J. Phys. Soc. Jpn. **71**, 725 (2002).
[9] S. Ikeda, N. Metoki, Y. Haga, K. Kaneko, T. D. Matsuda, A. Galatanu, and Y. Ōnuki, J. Phys. Soc. Jpn. **72**, 2622 (2003).
[10] K. Kaneko, N. Metoki, N. Bernhoeft, G. H. Lander, Y. Ishii, S. Ikeda, Y. Tokiwa, Y. Haga, and Y. Ōnuki, Phys. Rev. B **68**, 214419 (2003).
[11] N. Metoki, K. Kaneko, E. Colineau, P. Javorský, D. Aoki, Y. Homma, P. Boulet, F. Wastin, Y. Shiokawa, N. Bernhoeft, E. Yamamoto, Y. Ōnuki, J. Rebizant, and G. H. Lander, Phys. Rev. B **72**, 014460 (2005).
[12] F. Honda, N. Metoki, K. Kaneko, D. Aoki, Y. Homma, E. Yamamoto, Y. Shiokawa, Y. Ōnuki, E. Colineau, N. Bernhoeft, and G. H. Lander, Physica B **359-361**, 1147 (2005).
[13] D. Aoki, Y. Homma, Y. Shiokawa, E. Yamamoto, A. Nakamura, Y. Haga, R. Settai, T. Takeuchi, and Y. Ōnuki, J. Phys. Soc. Jpn. **73**, 1665 (2004).
[14] E. Colineau, P. Javorský, P. Boulet, F. Wastin, J. C. Griveau, J. Rebizant, J. P. Sanchez, and G. R. Stewart, Phys. Rev. B **69**, 184411 (2004).
[15] Y. Homma, S. Nasu, D. Aoki, K. Kaneko, N. Metoki, E. Yamamoto, A. Nakamura, S. Morimoto, H. Yasuoka, Y. Ōnuki, and Y. Shiokawa, Physica B **359-361**, 1105 (2005).
[16] E. Yamamoto, D. Aoki, Y. Homma, Y. Shiokawa, Y. Haga, A. Nakamura, and Y. Ōnuki, Physica B **359-361**, 1099 (2005).
[17] D. Aoki, Y. Homma, Y. Shiokawa, H. Sakai, E. Yamamoto, A. Nakamura, Y. Haga, R. Settai, and Y. Ōnuki, J. Phys. Soc. Jpn. **74**, 2323 (2005).
[18] E. Colineau, F. Wastin, P. Boulet, P. Javorský, J. Rebizant, and J. P. Sanchez, J. Alloys Compd. **386**, 57 (2005).
[19] E. Colineau, F. Wastin, and J. Rebizant, J. Phys.: Condens. Matter **18**, 411 (2006).
[20] S. Katano, N. Minakawa, N. Metoki, T. Osakabe, J. Suzuki, Y. Koike, and Y. Ishii, Appl. Phys. A **74**, S270 (2002).
[21] J. de Meulenaer and H. Tompa, Acta Crystallogr. **19**, 1014 (1965).
[22] N. W. Alcock, G. S. Pawley, C. P. Rourke, and M. R. Levine, Acta Crystallogr., Sect. A: Cryst. Phys., Diffr., Theor. Gen. Crystallogr. **28**, 440 (1972).
[23] A. L. Spek, J. Appl. Crystallogr. **36**, 7 (2003).
[24] L. J. Farrugia, J. Appl. Crystallogr. **32**, 837 (1999).
[25] P. J. Becker and P. Coppens, Acta Crystallogr., Sect. A: Cryst. Phys., Diffr., Theor. Gen. Crystallogr. **30**, 129 (1974).
[26] P. J. Becker and P. Coppens, Acta Crystallogr., Sect. A: Cryst. Phys., Diffr., Theor. Gen. Crystallogr. **30**, 148 (1974).
[27] P. J. Becker and P. Coppens, Acta Crystallogr., Sect. A: Cryst. Phys., Diffr., Theor. Gen. Crystallogr. **31**, 417 (1975).
[28] D. Aoki, H. Yamagami, Y. Homma, Y. Shiokawa, E. Yamamoto, A. Nakamura, Y. Haga, R. Settai, and Y. Ōnuki, J. Phys.: Condens. Matter **17**, L169 (2005).
[29] D. Aoki, Y. Homma, Y. Shiokawa, E. Yamamoto, A. Nakamura, Y. Haga, R. Settai, and Y. Ōnuki, J. Phys. Soc. Jpn. **73**, 2608 (2004).
[30] S. Ikeda, Y. Tokiwa, Y. Haga, E. Yamamoto, T. Ōkubo, M. Yamada, N. Nakamura, K. Sugiyama, K. Kindo, Y. Inada, H. Yamagami, and Y. Ōnuki, J. Phys. Soc. Jpn. **72**, 576 (2003).

[31] S. Ikeda, T. D. Matsuda, Y. Haga, E. Yamamoto, M. Nakashima, S. Kirita, T. C. Kobayashi, M. Hedo, Y. Uwatoko, H. Yamagami, H. Shishido, T. Ueda, R. Settai, and Y. Ōnuki, J. Phys. Soc. Jpn. **74**, 2277 (2005).

[32] G. H. Lander, *Handbook on the Physics and Chemistry of Rare Earths*, edited by K. A. Gschneidner, Jr., L. Eyring, G. H. Lander, and G. R. Choppin (Elsevier Science, 1993), Vol. 17, Chap. 117, p. 635.

[33] T. Maehira, T. Hotta, K. Ueda, and A. Hasegawa, Phys. Rev. Lett. **90**, 207007 (2003).

[34] T. Maehira, T. Hotta, K. Ueda, and A. Hasegawa, New J. Phys. **8**, 24 (2006).

[35] I. Opahle, S. Elgazzar, K. Koepernik, and P. M. Oppeneer, Phys. Rev. B **70**, 104504 (2004).

[36] A. Kiss and Y. Kuramoto, J. Phys. Soc. Jpn. **75**, 034709 (2006).

[37] I. Opahle, S. Elgazzar, V. D. P. Servedio, M. Richter, and P. M. Oppeneer, Europhys. Lett. **74**, 124 (2006).

[38] H. Onishi and T. Hotta, New J. Phys. **6**, 193 (2004).